Molecular Biology of the Cell
Vol. 11, 1789–1800, May 2000

Stage-Specific Expression and Targeting of Cyst Wall Protein–Green Fluorescent Protein Chimeras in *Giardia*

Adrian B. Hehl,* Matthias Marti, and Peter Köhler

Institute of Parasitology, University of Zürich, 8057 Zürich, Switzerland

Submitted December 6, 1999; Revised February 7, 2000; Accepted February 14, 2000
Monitoring Editor: Howard Riezman

In preparation for being shed into the environment as infectious cysts, trophozoites of *Giardia* spp. synthesize and deposit large amounts of extracellular matrix into a resistant extracellular cyst wall. Functional aspects of this developmentally regulated process were investigated by expressing a series of chimeric cyst wall protein 1 (CWP1)–green fluorescent protein (GFP) reporter proteins. It was demonstrated that a short 110 bp 5′ flanking region of the CWP1 gene harbors all necessary *cis*-DNA elements for strictly encystation-specific expression of a reporter during in vitro encystation, whereas sequences in the 3′ flanking region are involved in modulation of steady-state levels of its mRNA during encystation. Encysting *Giardia* expressing CWP1–GFP chimeras showed formation and maturation of labeled dense granule-like vesicles and subsequent incorporation of GFP-tagged protein into the cyst wall, dependent on which domains of CWP1 were included. The N-terminal domain of CWP1 was required for targeting GFP to regulated compartments of the secretory apparatus, whereas a central domain containing leucine-rich repeats mediated association of the chimera with the extracellular cyst wall. We show that analysis of protein transport using GFP-tagged molecules is feasible in an anaerobic organism and provides a useful tool for investigating the organization of primitive eukaryotic vesicular transport.

INTRODUCTION

Giardia duodenalis (syn. *G. intestinalis*, *G. lamblia*) is a flagellated protozoan parasite of medical significance because it is a major cause of waterborne enteric disease worldwide (Adam, 1991). The biology of this parasite is of particular interest because it represents one of the earliest branching lineages of eukaryotic descent, based on phylogenetic analysis of ribosomal and protein coding sequences (Sogin *et al.*, 1989; Leipe *et al.*, 1993; Gupta *et al.*, 1994; Drouin *et al.*, 1995; Roger *et al.*, 1999). *Giardia* also lacks organelles typical for higher eukaryotes such as mitochondria and peroxisomes. Asexually dividing, motile trophozoites colonize the upper intestine of humans and other mammals, where they attach to the intestinal epithelium (Adam, 1991). Encysting *Giardia* trophozoites undergo a series of developmental changes in the course of which they synthesize, export, and assemble an extensive fibrillar extracellular matrix composed of proteins but also a large proportion of carbohydrate, mainly in the form of *N*-acetylgalactosamine (Manning *et al.*, 1992). Formation of environmentally resistant cysts is a key step in *Giardia* development as in other eukaryotic pathogens (Eichinger, 1997; Taratuto and Venturiello, 1997; Dubey *et al.*, 1998) that has not been well characterized on a molecular level. Therefore, a better understanding of the mechanisms that govern stage-specific regulation of genes and the synthesis, transport, and assembly of the cyst wall is needed.

Several genes that are up-regulated during *Giardia* encystation have been identified recently by biochemical approaches, molecular genetics, or metabolic studies (Ellis *et al.*, 1996; Que *et al.*, 1996; Steimle *et al.*, 1997; Bulik *et al.*, 1998; Paget *et al.*, 1998; Van Keulen *et al.*, 1998; Knodler *et al.*, 1999). Among these, cyst wall protein (CWP) 1 and CWP2 constitute major components of an extracellular cyst wall (Lujan *et al.*, 1995b; Mowatt *et al.*, 1995), the function of which has not been determined. These proteins are targeted to the secretory apparatus by their predicted hydrophobic leader sequence where they apparently associate covalently via disulfide bonds shortly after their synthesis. Proteins and carbohydrates destined for the cyst wall are transported by a novel class of as yet undefined vesicles termed encystation-specific vesicles (ESVs) (Reiner *et al.*, 1989, 1990, 1993). Their contents are secreted and assembled into a fibrillar, tough structure, which protects the parasite against environ-

* Corresponding author. E-mail address: ahehl@vetparas.unizh.ch.
Abbreviations used: CWP, cyst wall protein; ESV, encystation-specific vesicle; GFP, *Aequorea victoria* green fluorescent protein; RT, reverse transcription; UTR, untranslated region.

mental stress and allows passage through the stomach during infection of a new host.

Although typical Golgi structures (i.e., stacks of flattened cisterna) have not been observed in *Giardia*, there are several lines of biochemical and immunocytochemical evidence that suggest the presence of a Golgi-like system for both constitutive and regulated protein transport, albeit some key functions appear to be restricted to cells in the process of encystation (Lujan *et al.*, 1997). The observation that generation of ESVs occurs only in encysting cells (Reiner *et al.*, 1990) further supports the notion that, in addition to the cyst wall components, some structures and functions of the corresponding transport and secretion machinery may be developmentally regulated as well.

The analysis of gene regulation and protein transport in *Giardia* has been severely hampered by a lack of suitable molecular genetic methods. Stable transformation and expression of reporter proteins have been demonstrated only recently in trophozoites, using a viral system (Wang *et al.*, 1995; Yu *et al.*, 1995, 1996a,b) and subsequently also by electroporation of plasmid-based vectors (Yee and Nash, 1995; Singer *et al.*, 1998; Sun *et al.*, 1998). As an initial step toward the complete molecular dissection of regulated protein trafficking in this ancient eukaryotic protozoan, we describe for the first time in an anaerobic organism a model for the study of stage-specific expression, protein targeting, and transport using green fluorescent protein (GFP) as a reporter.

MATERIALS AND METHODS

Cell Culture and Transfection

Trophozoites of the *G. duodenalis* WB (Smith *et al.*, 1982) clone C6 were grown vegetatively in TYI-S-33 medium supplemented with 10% adult bovine serum and bovine bile as described previously (Bruderer *et al.*, 1993). For induction of encystation in vitro, we used the two-step method as described (Boucher and Gillin, 1990).

Electroporation of vector DNA into cultured trophozoites was performed essentially as described in Yee and Nash (1995) using 15 μg purified plasmid DNA per 10^7 cells. For selection of stable transformants the parasites were maintained in TYI-S-33 culture medium containing the antibiotic G418 (Sigma, St. Louis, MO) at a concentration of 135 μg/ml. Proliferating G418-resistant parasites were apparent after 2–3 d. Transgenic parasites were grown to confluency and subsequently passaged every other day with continuous antibiotic selection.

Plasmid Vector Construction

Vectors for transfection were designed as double cassettes with a constant part containing a bacterial neomycin resistance gene under the control of the *Giardia RAN* gene flanking sequences (Chen *et al.*, 1994; Sun *et al.*, 1998) (see Figure 1). The *NEO*-resistance cassette was constructed by PCR amplifying 982 bp from the *RAN* locus (GenBank accession number U02589) including short flanking sequences with primers RAN-s and RAN-as. The fragment was subcloned into the *Xba*I and *Sal*I sites of pBluescript KS(−) (Stratagene, La Jolla, CA) and used as a template for inverse PCR amplification of *RAN* flanking sequences including the entire vector with primers RAN-ias and RAN-is. The fragment was cut with restriction enzymes *Bgl*II and *Eco*RI and ligated with the amplified 795-bp neomycin acetyl transferase gene fragment (primers NEO-s and NEO-as) containing the corresponding restriction sites, giving rise to a construct pRAN-NEO.

The *CWP1* locus was PCR-amplified from genomic DNA using primers CWP1-s and CWP1-as, cut with *Eco*RI, and ligated into pBluescript. 5′ (120 bp) and 3′ (173 bp) flanking sequences for ligation with the *GFP* gene were again obtained by inverse PCR using the downstream sense primer CWP-C1–4s containing a *Pac*I site and five different upstream antisense primers, CWP-C0-as, CWP-C1-as, CWP-C2-as, CWP-C3-as, and CWP-C4-as, each containing a *NsiI* site that also supplied the translation start site. In-frame ligation of a *NsiI* and *Pac*I GFP fragment gave rise to chimeric genes with progressive addition of CWP1 domains to the N-terminal side of GFP. GFP variant m-GFP-5 (Siemering *et al.*, 1996) was obtained from the Medical Research Council, Cambridge, UK via Dr. K. Kim.

A control vector pC0-GFP contained only *CWP1* flanking regions upstream and downstream of the *GFP* gene but no sequences from the *CWP1* ORF. In the pC1-GFP construct we fused the *CWP1* sequence coding for the N-terminal 16 amino acids including a hydrophobic stretch and a predicted signal peptide cleavage site between Ala(14) and Leu(15) (domain I) to the *GFP* ORF. An additional stretch coding for the mature N-terminal 53 aa containing three cysteine residues was added in pC2-GFP, and for pC3-GFP a region of 120 aa containing the five leucine-rich repeats (LRRs) (domain III) was included. Plasmid pC4-GFP contained the full-length ORFs of both *CWP1*, coding for domains I–IV, and *GFP*. Construct pC0-PP2 was generated by removing the *CWP1* 3′ flanking sequence by restriction digestion with *Pac*I and *Bam*HI, and ligation of a 505-bp fragment PCR-amplified with primers PP2-s and PP2-as. The *PP2* fragment contained the 3′ flanking region of the *Giardia* protein phosphatase 2C gene homolog, including a canonical poly(A) addition site AGTAAA starting 18 bp downstream of the *PP2* stop codon.

The neomycin resistance cassette and *CWP1–GFP* chimeric genes were combined on a single plasmid in a head-to-head arrangement. The *CWP1–GFP* fragments were purified after restriction enzyme digestion with *Eco*RV and *Not*I and ligated into the linearized pRAN-NEO plasmid containing a blunted *Xba*I and a *Not*I site adjacent to the *RAN* promoter sequence.

Synthetic Oligonucleotide Primers (5′–3′ Orientation)

Vector Construction. CWP-C0-as CG*ATGCAT*CCCTGATATTTTATTTCT; CWP-C1-as GT*ATGCAT*AGTGAGGGCAAGGGCAGAA; CWP-C2-as CG*ATGCAT*ATCCAGGGCGATAACGTAGT; CWP-C3-as CG*ATGCAT*AAGGTAGGGGAGCGTC; CWP-C4-as CGATGCATAGGCGGGGTGAGGCAGT; CWP-C1–4s CG*TTAATTAA*CCTAAACGGTAGCCACGA; CWP1-s AT*GAATTC*CTAGCCACGCATGGGCTGT; RAN-i-as CG*AGATCT*GCTACTCTCGGTTCCTGGGT; RAN-i-s GC*GAATTC*GCAGGCCTTTGATGACT; RAN-as AC*GTCGAC*GATAGCGCATTTACTACCT; RAN-s CG*TCTAGA*GCCGCTTCAATGACAGA; NEO-as CA*GAATTC*TCAGAAGAACTCGTCAAGA; NEO-s CG*AGATCT*ATGATTGAACAAGATGGA; PP2-s CG*TTAATTAA*TGCGTCTATGTCAGCAAGT; PP2-as AC*GGATCC*GCGACGAAATGCGTCCTTGA.

Reverse Transcription-PCR. K-Ad CCGGAATTCGGTACCTCTAGA; K-An CCGGAATTCGGTACCTCTAGA(T_{18})K; NEO-s-q ATGCCTGCTTGCCGAATATCA; GFP-s-q GACGGGAACTACAAGACACGT; GDH-s-q AGGTCCTCACCTTCTCAGACT; CWP-s-q CTGGTACATGAGTGACAACGCT; PP2-s-q CACGTTGGGAGACCATTGCA.

Protein Analysis

Cells were harvested for gel electrophoresis by quick-chilling culture tubes in an ice/NaCl slush, inverting 10 times, and centrifugation at 1000 × *g*. The cell pellets were washed once in ice-cold PBS and counted. SDS sample buffer was added to obtain a uniform density of 5×10^5 cells/10 μl volume, and samples were immedi-

ately boiled for 3 min. If not otherwise stated, DTT was added to a final concentration of 7.75 mg/ml before boiling. SDS-PAGE on 10% polyacrylamide gels and transfer to nitrocellulose membranes was performed according to standard techniques (Ausubel *et al*., 1994). Filters were blocked in 5% dry milk/0.5% TWEEN-20/PBS and incubated with polyclonal rabbit antiserum to GFP (Clontech, Cambridge, UK) diluted in blocking solution. Bound antibodies were detected with horseradish peroxidase-conjugated goat anti-rabbit IgG (Bio-Rad, Hercules, CA) and developed using enhanced chemiluminescence (Amersham, Arlington Heights, IL).

RNA Preparation and Analysis of cDNA Levels by Reverse Transcription-PCR

Total RNA from wild-type and transgenic trophozoites or encysting cells at 15 h after induction was prepared as described above. Cell pellets were resuspended in a minimal volume of ice-cold PBS and dissolved in Ultraspec RNA solution (Biotecx Laboratories, Houston, TX), and total RNA was prepared according to the protocol supplied by the manufacturer. Total RNA concentrations for each preparation were determined in a Uvikon 860 photospectrometer (Kontron Instruments, Watford, United Kingdom). For reverse transcription-PCR (RT-PCR), 3 μg total RNA was reverse-transcribed with 100 ng of primer K-An and 50 U of SuperScript II reverse transcriptase (Life Technologies, Gaithersburg, MD) at 45°C in 25 mM Tris-HCL, pH 8.3, 75 mM KCl, 3 mM $MgCl_2$, 10 mM DTT, and 500 μM dNTP (Clontech). The reaction was incubated at 45°C for 50 min and heat-inactivated at 70°C followed by digestion with 10 U RNAse H (Life Technologies) for 20 min at 37°C. Single-stranded cDNA was purified with the GlassMAX DNA isolation spin cartridge system (Life Technologies). Single-stranded cDNA corresponding to 0.12 μg of total RNA and serial fivefold dilutions were used as template for PCR amplification with 10 pmol each of primer K-Ad and gene-specific sense primers. Primer sequences were chosen to amplify fragments of between 400 and 500 bp from each cDNA, containing the end of the gene ORF and the complete 3′ untranslated region (UTR). Reaction conditions were 10 mM Tris-HCl, pH 8.3, 50 mM KCl, 2 mM $MgCl_2$, 0.001% gelatin, 200 μM each dNTP, and 1.5 U recombinant *Taq* polymerase (Life Technologies). Thermal cycling conditions were as follows: "hot start cycle," 94°C, 5 min; 80°C, 2 min; (addition of *Taq* polymerase to the reaction) 64°C, 1 min; 72°C, 1 min, followed by 21 cycles (linear range between 15 and 25 cycles) at 94°C, 30 s; 64°C, 1 min; 72°C, 1 min; with a final extension at 72°C for 10 min. PCR products were separated on 6% polyacrylamide gels or 1.3% agarose gels, the latter containing the appropriate amount of SYBR Green I (Molecular Probes, Eugene, OR). Polyacrylamide gels were poststained with SYBR Green I for 20 min. Data collection was performed on a Fluorimager (Molecular Dynamics, Sunnyvale, CA), and the data were analyzed with ImageQuant software (Molecular Dynamics). Negative controls were 1) omission of enzyme in the RT reaction, 2) omission of template cDNA in the PCR reaction, 3) PCR reaction for 30 cycles using only a single primer, and 4) RNAse A digestion before the RT reaction.

For the determination of poly(A) addition sites, 3′ rapid amplification of cDNA end fragments from the mRNA of endogenous *CWP1* and transfected *CWP1–GFP* constructs were generated using the conditions described above for RT-PCR and 30 cycles of PCR amplification. PCR products were cloned into the pCR2-Topo vector (Clontech), and inserts were analyzed by dye termination sequencing (Microsynth GmbH, Balgach, Switzerland).

Microscopy

Trophozoites and encysting cells were harvested as described above. To allow GFP maturation, harvested cultures were dispensed in 1-ml aliquots into 24-well culture dishes in encystation medium and stored exposed to air atmosphere for several hours between 0 and 4°C. Alternatively, 100-μl aliquots of cell suspension were oxygenated for 30 min on coverslips in an enriched O_2 atmosphere at 37°C. Cells in suspension were collected at 300 × *g* (4°C). Pellets of live, unfixed cells were either directly resuspended in microscopy embedding solution (Difco, Detroit, MI) and sealed under coverslips with paper glue or resuspended in encystation medium, transferred to round poly-lysine-coated coverslips, and incubated in a humid 5% CO_2 atmosphere at 37°C for 30–60 min. Excess fluid was drained from the coverslips, and reattached *Giardia* were inverted onto a drop of embedding solution. For live cell observation, embedding solution was omitted. Oxygenated parasites were also washed in ice-cold PBS and fixed in cold 2% formaldehyde before embedding for microscopy. Enriched fractions of water-resistant cysts were prepared by incubating harvested parasites in ice-cold water for 1 h, washing once with water, and collecting cysts at 300 × *g* for 10 min. Nuclear staining was performed by addition of 1 μg/ml DAPI (Boehringer Mannheim, Indianapolis, IN) to the parasite suspension before embedding. For specific labeling of Golgi membranes, oxygenated cells were fixed with 2% paraformaldehyde in PBS and washed in cold HEPES-buffered DMEM (HMEM). BODIPY-TR–ceramide (Molecular Probes) was complexed to defatted BSA (DF-BSA) as described in Pagano and Martin (1988) and incubated with the cells at 5 nM/ml in HMEM on ice for 30 min. Cells were washed once with cold HMEM and four to five times for 30 min in TYI-S-33 medium supplemented with 10% adult bovine serum at room temperature to remove excess stain.

For treatment with brefeldin A (Fluka, Buchs, Switzerland), oxygenated cells were washed and incubated for 40 min at 37°C in TYI-S-33 medium supplemented with 10% adult bovine serum including brefeldin A dissolved in DMSO (Fluka) at 50 μg/ml or DMSO alone as a control.

Microscopy was performed with a Zeiss Axiovert S100 fluorescence microscope equipped with a CCD camera (Hamamatsu C5810; Hamamatsu Photonics, Hamamatsu City, Japan). Data were collected and processed using Adobe Photoshop. Image processing included merging of DAPI and GFP signals into a single image and linear contrast stretch. Confocal microscopy was performed using a Leica (Bensheim, Germany) confocal laser scanning microscope with the appropriate filter sets. A series of 20 optical sections with an approximate z-distance of 0.3 μm were performed for each cell. Image processing (linear contrast stretch and merging of DAPI, GFP, and DIC signals) was performed with the Imaris program (Bitplane, Zurich, Switzerland). A z-plane correction factor for the DIC images was determined and applied. For Figure 7 the blue DAPI signal was converted into a red color for better contrast and visibility in images of individual optical sections. Three-dimensional reconstruction of optical sections was performed with the Imaris software suite. Perspective views were rotated to show an aspect that provides an optimal view of nuclei and transport vesicles containing GFP. The dorsal–ventral axis corresponds to the *z*-axis of individual optical sections, and the orientation of cells in the three-dimensional images is indicated accordingly in Figure 7.

RESULTS

Stage-specific Control of CWP1 Expression Is Mediated by 5′ cis*-DNA Elements*

We wanted to determine whether 1) the known 5′ flanking sequence upstream of the transcription initiation site of ~110 bp contained a promoter that is able to drive expression of a reporter gene, 2) this flanking region contained the necessary *cis*-DNA elements for stage-specific control of expression, and 3) the *CWP1* 3′UTR and flanking sequences contributed in any way to expression control. We constructed a vector pC3-GFP (Figure 1) that contained a chimeric *CWP1–GFP* gene flanked by upstream *CWP1* sequences and 170 bp of sequence downstream of the

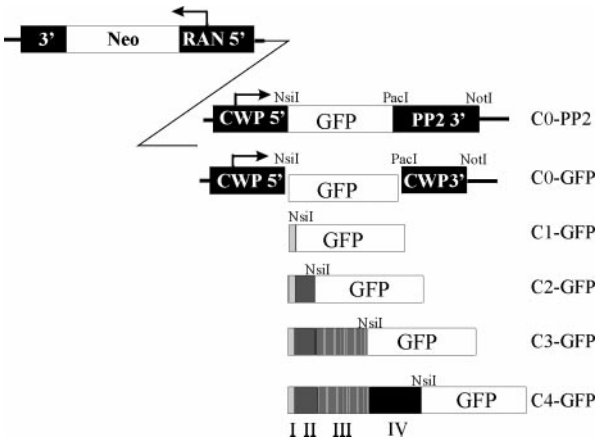

Figure 1. Schematic representation of plasmid vectors used for stable transformation of *Giardia* trophozoites. A *RAN-neo* cassette conferring constitutive G418 resistance is cloned immediately adjacent to a recombinant *CWP1* locus in a head-to-head conformation on a pBluescript backbone. All four domains of CWP1 (I–IV) are sequentially added to the N-terminal side of a *GFP* reporter gene. In construct pC0-PP2, the *CWP1* 3′ flanking sequence was replaced by that of the *Giardia PP2* gene. CWP1 domains are indicated by roman numerals. Promoters and corresponding direction of transcription are represented by bent arrows.

translation termination codon. This and all other constructs used in this study were maintained stably as episomes under selection for G418 resistance.

Levels of C3-GFP protein and mRNA were measured before and after induction of encystation in vitro. *C3-GFP* mRNA in stably transfected cells determined by semiquantitative RT-PCR was increased >100-fold in 15-h encysting cells compared with the trophozoite control (Figure 2A). Endogenous *CWP1* mRNA, determined as a positive control, was approximately five times more abundant than the heterologous *C3-GFP* mRNA and showed equivalent kinetics of induction, i.e., >100-fold induction during encystation. *GDH* mRNA levels, which vary only slightly during encystation (Mowatt *et al.*, 1995), were determined to ensure that equal amounts of cDNA were being compared. *NEO*-specific primers were also used to show that a comparable amount of transcript was present from the constitutively expressed neomycin-resistance gene also present on the plasmid. Sequencing of 3′ rapid amplification of cDNA end products showed that *C3-GFP* mRNAs were correctly processed by addition of a poly(A) tail at the same position as endogenous *CWP1* mRNA (nt 773; GenBank accession number U09330). Western blot analysis of total protein incubated with anti-GFP antiserum revealed major bands of 46/48 kDa and 39 kDa in 24-h encysting cells that were not detectable, or only weakly detectable, in trophozoites or cells during preencystation (Figures 2B, 4). The detected 46/48-kDa double band was in good agreement with the predicted size of a full-length C3-GFP chimeric protein of 47 kDa, whereas the smaller band of ~40 kDa, whose intensity varied considerably between experiments, may be either a specific cleavage product or the result of protein degradation during lysate preparation. Detectable levels of GFP were seen in Western blots 5 h after stimulating encystation in vitro and peaked

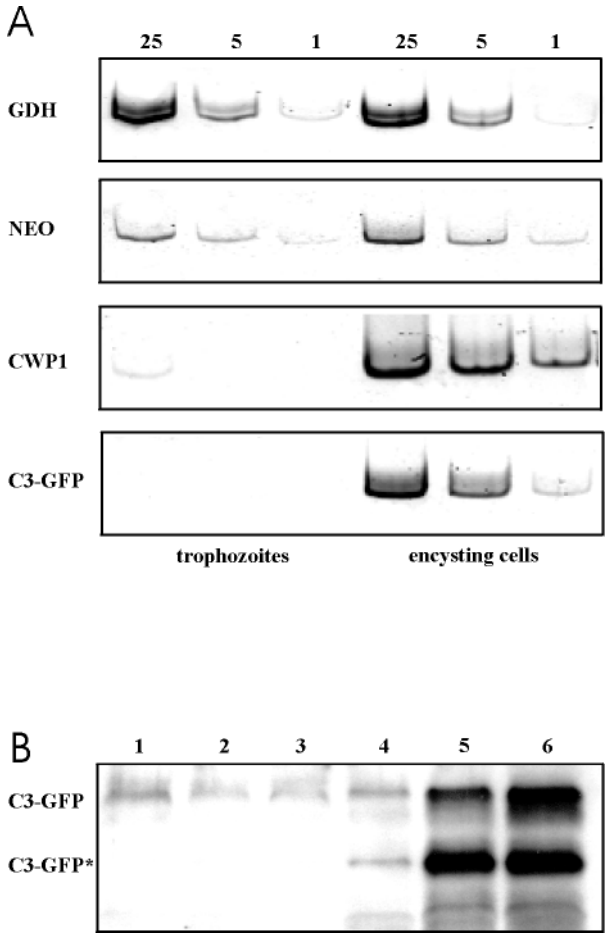

Figure 2. (A) Stage-specific expression of CWP1–GFP reporter. Semiquantitative RT-PCR was performed. Gene-specific products amplified from trophozoites (left three lanes) and encysting cells at 15 h after induction (right three lanes) were separated on polyacrylamide gels and stained with SYBR Green. Fivefold serial dilutions of single-stranded template cDNA, produced from equal amounts of total RNA with primer K-An, was used in the PCR reaction (25, 5, and 1×). Product detected in 25× is equivalent to ss-cDNA produced from 0.12 μg total RNA. *GDH* and *CWP1* represent RT-PCR products of the corresponding endogenous mRNAs as a control for equal template concentration and efficient induction of encystation, respectively. Stage-regulation of *C3-GFP* is equivalent to that of endogenous *CWP1* mRNA. (B) Western blot probed with an anti-GFP antibody showing kinetics of C3-GFP induction after stimulation of encystation in vitro. Lane 1, 0 min; lane 2, 15 min; lane 3, 1 h; lane 4, 5 h; lane 5, 7 h; lane 6, 24 h after induction. The full-length product of the C3-GFP is indicated. The asterisk indicates a major band representing a breakdown product of C3-GFP.

around 24 h (Figure 2B), in agreement with previously observed kinetics of CWP1 expression during encystation (Mowatt *et al.*, 1995). Stage-specificity was shown to be independent of sequences in the *CWP1* ORF, because C0-GFP was also expressed in a stage-specific manner (see below and Figure 4). Background levels of endogenous CWP1 expression or the chimeric proteins used in this study in normal trophozoite culture can be attributed to spontaneous initia-

tion of encystation of a small number of cells, rather than to a general leakiness of the *CWP1* promoters.

Modulation of Steady-state CWP1 mRNA Levels by 3′UTR Sequences

To prove that 5′ flanking sequences were necessary and sufficient for encystation-specific reporter mRNA expression, we replaced the *CWP1* downstream flanking region in the construct pC0-GFP with that of a constitutively expressed *Giardia* protein phosphatase 2C (PP2) gene (GenBank accession number L27221). C0-PP2 mRNA levels in transformed trophozoites and encysting cells were compared by semiquantitative RT-PCR as described above. As controls we also assessed mRNA levels of endogenous *CWP1* and *PP2*. We found that stage-specific expression of the reporter mRNA was independent of the 3′UTR used in the construct (Figure 3A). The relative increase of mRNA levels in cells 15 h after induction was comparable for *C0-GFP*, *C0-PP2*, and endogenous *CWP1*, whereas endogenous *PP2* mRNA expression was unchanged. This shows that induction of *CWP1* mRNA synthesis during encystation is independent of 3′ flanking sequences.

Interestingly, levels of *C0-PP2* mRNA determined in semiquantitative RT-PCR were found to be 40–50 times higher than those of *C0-GFP* (Figure 3A). The amount of *NEO* mRNA transcribed from the same plasmid, on the other hand, was comparable to that found in parasites transformed with pC0-GFP, indicating that this effect was not due to an increased replication of pC0-PP2. A similar absolute increase in protein synthesis compared with the C0-GFP product was also seen in Western blot analysis of cells transformed with pC0-PP2 (Figure 3B), suggesting that replacement of the 36-base 3′UTR of *CWP1* in the reporter construct leads to unchecked production of the corresponding product.

Expression of CWP1–GFP Chimeric Proteins

CWP1 can be divided into four domains according to structural information derived from the amino acid sequence (see also MATERIALS AND METHODS). Characteristic for a secreted protein, an amino-terminal stretch of hydrophobic amino acids with a predicted signal sequence cleavage site is found (domain I). The 53 aa spanning domain II borders on a central portion of CWP1 (domain III) consisting of five degenerate 24 aa LRRs. Domain III is of particular interest in connection with the formation of the fibril structures in the *Giardia* cyst wall because LRRs are known to promote noncovalent protein–protein interactions. Finally, domain IV constitutes a cysteine-rich C-terminal region of 50 aa, which had been implicated in the covalent linkage of CWP1 with CWP2 via disulfide bridges. To investigate functional aspects of these four domains, expression vectors for GFP-tagged chimeric genes containing successive additions of the four structural domains of CWP1 (Figure 1) under the control of CWP1 promoter sequences were generated. In Western blot analysis (trophozoites; 24-h encysting cells) the C0-GFP product (GFP alone) was expressed stage-specifically (Figure 4) and did not associate significantly with other proteins under nonreducing conditions (Figure 5). Cells transformed with pC1-GFP containing the CWP1 leader sequence and predicted cleavage site showed an unexpected

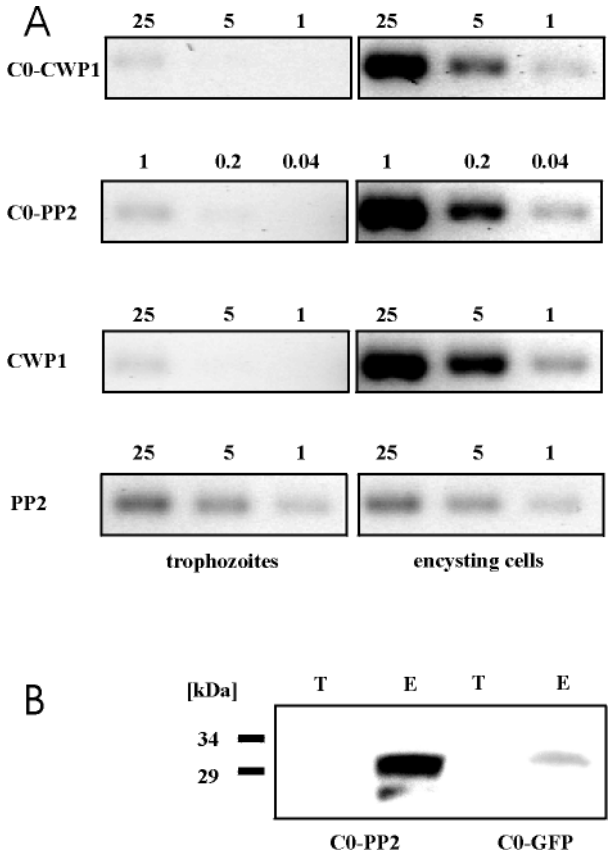

Figure 3. (A) The influence of the CWP1 3′UTR on steady-state mRNA levels. Stage-specific induction of reporter mRNA expression is independent of the 3′ flanking region. Semiquantitative RT-PCR using total RNA isolated from trophozoites (left panels) and cells 15 h after induction (right panels) transformed with constructs pC0-GFP or pC0-PP2. Serial dilutions of ss-cDNA templates are indicated at the top of each panel; 25× corresponds to cDNA produced from 0.12 μg total RNA. Top panel, C0-GFP-specific amplification products; second panel, C0-PP2-specific product; the maximal amount of cDNA template used in this reaction is 25-fold less than for all the other RT-PCR experiments because of the high concentration of *C0-PP2* mRNA in the cells. Controls, stage-regulated endogenous CWP1 (third panel) and constitutive endogenous PP2 (bottom panel) RT-PCR products amplified from pC0-PP2–transformed parasites. (B) Expression levels of GFP produced from pC0-PP2 are elevated with respect to those produced from pC0-GFP in encysting cells. Equal numbers of stably transfected trophozoites (T) and encysting cells (E) were lysed, separated on reducing SDS-PAGE, and transferred to filters. GFP was detected with a rabbit anti-GFP serum. Molecular mass markers are indicated.

phenotype. We were able to maintain the construct in trophozoites but were not successful in our attempts to produce cysts with this population. Although trophozoites grew at a normal rate, the cells swelled and died during preencystation. The chimeric gene was designed to specifically exclude the first cysteine residue of CWP1 at position 17 of the proprotein. One possible explanation for the lethal phenotype is that the prediction of the cleavage site for the signal sequence by computer programs such as PSORT, both for CWP1 and the chimeric protein, were inaccurate. A

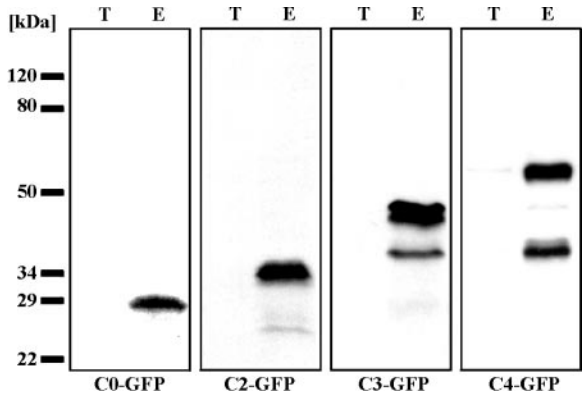

Figure 4. Stage-specific expression of CWP1–GFP chimeric proteins. Western blot analysis of total protein from transformed trophozoites (T) and encysting cells (E) separated by SDS-PAGE and probed with anti-GFP antiserum. Top bands in each lane represent full-length products of the respective chimeras or GFP alone (C0-GFP). Parasites transformed with pC1-GFP exhibited an encystation-specific lethal phenotype and are not shown. Migration of molecular mass markers is indicated on the left. Encystation-specific expression of C0-GFP demonstrates that stage-specificity is independent of sequences in the CWP1 ORF.

noncleavable leader sequence could lead to a failure to clear the product at ER translocation sites and eventually lead to cell death. Products of pC2-GFP revealed a major double band around 42 kDa in reducing gels (Figure 4) and a number of additional bands in the range of 60–210 kDa in nonreducing conditions (Figure 5). The latter represent covalent linkage of the chimera, presumably with endogenous CWP2, via disulfide cross-linking of the three cysteines in domain II of C2-GFP. Parasites transformed with the C3-GFP gene, containing CWP1 domains I–III, showed a doublet of ~46/48 kDa in Western blots with anti-GFP antiserum (Figure 4). Under nonreducing conditions a majority of the chimera appeared covalently linked to other proteins (Figure 5). The construct pC4-GFP contained the entire CWP1 gene in frame with GFP. In Western blots a major double band migrating at ~54 kDa was detected with anti-GFP antibodies (predicted mass: 53 kDa) under reducing conditions (Figure 4). In nonreducing conditions virtually all of the C4-GFP product was present as high molecular weight complexes (Figure 5).

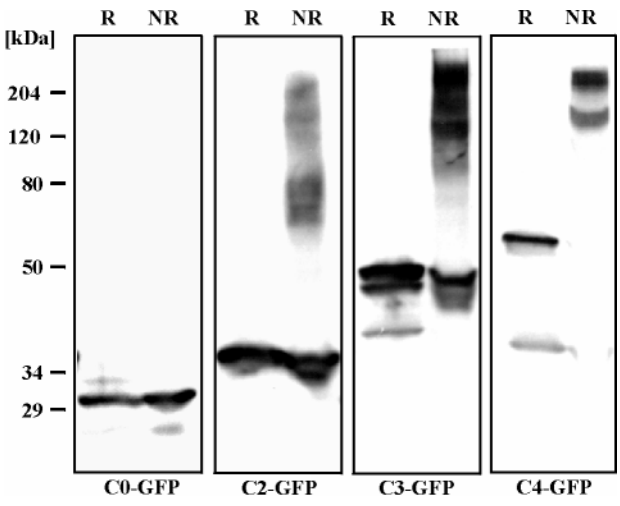

Figure 5. CWP1–GFP chimeras form covalent interactions with other proteins, presumably CWP2. A Western blot of total protein from encysting parasites was probed with anti-GFP antiserum. Equal amounts of protein were separated on SDS-PAGE with DTT as reducing agent (R) or under nonreducing conditions (NR). All three chimeric proteins form disulfide-linked high molecular weight complexes under nonreducing conditions (NR). GFP protein alone (C0-GFP) does not show any interaction with other proteins. Migration of molecular mass markers is indicated on the left.

This analysis confirms stage-specific expression of all chimeras with the exception of C1-GFP. Major bands with the exception of C0-GFP appeared as closely migrating doublets, indicating a possible posttranslational processing event in addition to the cleavage of the N-terminal CWP1 signal sequence. Additional minor low molecular weight bands, possibly degradation products because their intensities varied between experiments, were observed for C3-GFP and C4-GFP. A similar phenomenon has been observed previously with antibodies to endogenous CWP1 and CWP2 (Lujan *et al.*, 1995b). The increasing length of CWP1 sequences included in the chimeric proteins correlated with the stability of covalent protein–protein interaction in nonreducing conditions, ranging from no interaction (C0-GFP) to complete cross-linking (C4-GFP) (Figure 5). This suggests that cysteines in all three domains of the mature CWP1 are engaged in the formation of intermolecular bonds.

Targeting of CWP1–GFP Chimeric Proteins to the Cyst Wall

To determine the subcellular localization of the GFP-tagged CWP1 chimeras during the cyst-forming process (5-h encysting cells; mature cysts), GFP expression was analyzed by fluorescence microscopy of unfixed, embedded parasites. Live motile cells showed a distribution of GFP signal that was indistinguishable from that of embedded or fixed parasites. Morphological criteria for the identification of cysts were oval cell shape, lack of flagella, refractile cyst wall structure in bright field, and more than two visible nuclei when viewed with the DAPI filter set. An initial lack of fluorescence attributable to the anaerobic culture conditions was overcome by harvesting the parasites and keeping them in the cold in normal medium exposed to atmospheric air for several hours (see MATERIALS AND METHODS).

C0-GFP was found in a cytoplasmic location, in both encysting trophozoites and mature cysts (Figure 6A, panels A and B), reflecting the lack of a hydrophobic leader sequence for targeting GFP to the secretory pathway. GFP in encysting pC2-GFP–transformed parasites localized to distinct vesicular structures in the cytoplasm (Figure 6A, panel C), indicating that the C2-GFP chimeric protein is capable of entering the secretory pathway, presumably by virtue of its N-terminal signal sequence. Identifiable cyst forms, however, did not contain any GFP-labeled cytoplasmic vesicles and showed only very light diffuse GFP signal, if any, in the periphery of the cells (Figure 6A, panel D). The C3-GFP chimera also localized to vesicular structures of encysting cells but is now also found associated with the wall of fully

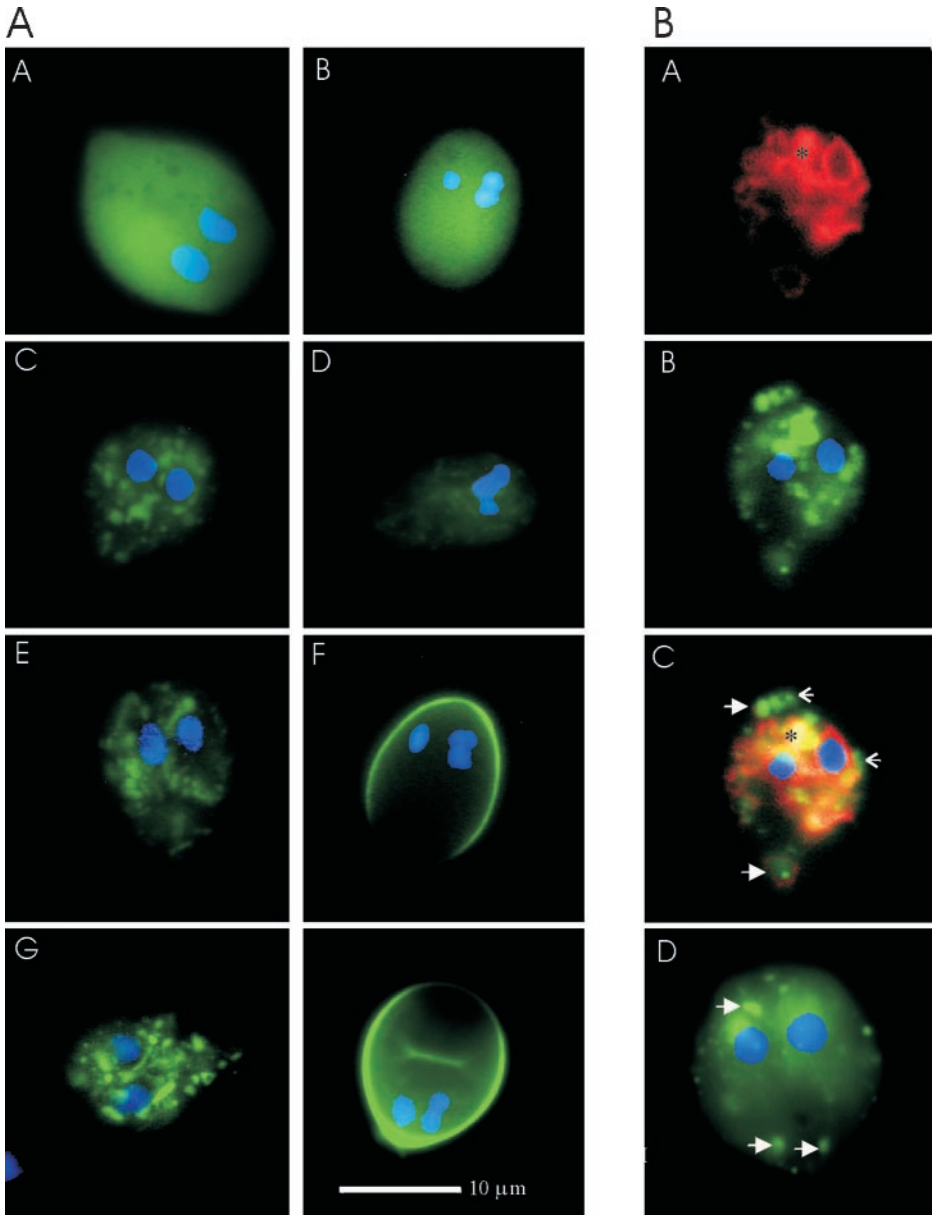

Figure 6. (A) Subcellular localization of CWP–GFP chimeric proteins in encysting cells is shown 5 h after induction (panels A, C, E, and G) and in fully formed cysts (panels B, D, F, and H) observed by fluorescence microscopy. Nuclei stained with DAPI appear blue and were merged with the GFP image. Panels A and B, C0-GFP (GFP alone); panels C and D, C2-GFP containing domains I and II of CWP1; panels E and F, C3-GFP containing the LRRs; panels G and H, the complete chimera C4-GFP. (B) Identification of putative Golgi and post-Golgi vesicles containing cyst wall material. Colocalization of fluorescent C4-GFP with BODIPY-TR–ceramide in Golgi membranes. Panel A, staining of Golgi membranes in an encysting cell; panel B, GFP signal in vesicular compartments of the same cell; panel C, merged image showing colocalization of both signals predominately in the perinuclear region (asterisk, yellow stain) but also in peripheral areas. Peripheral vesicles that are weakly or only partially labeled with BODIPY-TR–ceramide (full arrows) may be transitional compartments. GFP-labeled putative post-Golgi compartments that did not stain with BODIPY-TR–ceramide are indicated with pointed arrows. Panel D, most of the GFP label redistributes to an area around the nuclei in live brefeldin A-treated encysting cells, but putative post-Golgi vesicles remain intact (arrows).

formed cysts (Figure 6A, panels E and F). This shows that domain III of CWP1 containing five LRRs is necessary for localizing the protein to the cyst wall structure itself. Identification of a strong GFP label in cyst walls provided evidence that transport of the CWP–GFP chimera is correct and the protein is not misdirected in the cell. Although we do not have the means to directly demonstrate the correct targeting of GFP-tagged protein during earlier stages of encystation, the apparently complete translocation of ESV contents into the wall structure of viable cysts supports our conclusion that expression of the chimeric protein does not significantly perturb the physiology of the transport machinery. Localization of the C4-GFP product in both stages of development (Figure 6A, panels G and H) was found to be indistinguishable from that of the C3-GFP protein. Thus, although it was possible to attribute a function to domains I/II and III of CWP1, inclusion of the C-terminal domain IV in construct C4-GFP did not have a detectable effect on the subcellular localization of the chimeric protein.

To date there are no specific antibodies available for Golgi marker proteins in *Giardia*, which makes it difficult to determine whether CWPs transit through the Golgi before being sequestered into ESVs. In an attempt to colocalize C4-GFP with Golgi vesicles, we therefore visualized Golgi membranes by fixing transformed cells and labeling with BODIPY-TR–ceramide during encystation. Labeled ceramide analogues exhibit a high affinity for Golgi membranes in cells of higher eukaryotes (Pagano, 1989). Although it has not been rigorously proven that this is also the case in *Giardia*, Lujan and coworkers (1995a) have used this tech-

nique to identify a perinuclear structure that is only present in encysting cells and is thought to constitute the *Giardia* Golgi. After incubation of parasites with BODIPY-TR–ceramide followed by extensive backwashes, only internal membranes remained fluorescently labeled. In fluorescence microscopy studies we found vesicles containing GFP-tagged CWP1 that colocalized with BODIPY-TR–ceramide predominantly in perinuclear regions (Figure 6B, panels A–C). Because membranous structures in this area of the cell appear very dense and seem to be closely stacked, as also seen in electron microscopy studies (McCaffery and Gillin, 1994), it remained uncertain whether perinuclear colocalization with GFP was coincidental or indeed represented Golgi vesicles containing tagged CWP1. In more peripheral areas of the cytoplasm, however, we observed GFP-containing vesicles that were clearly outlined by the marker lipid. Others, for the most part close to the plasma membrane, were not labeled or only partially labeled with BODIPY-TR–ceramide. These latter vesicles are suggestive of more mature ESVs belonging to a putative post-Golgi compartment. This conjecture was further supported by incubation of live cells with brefeldin A during encystation. The treatment caused most of the GFP-labeled vesicles to disperse and GFP to redistribute to the area surrounding the nuclei, demonstrating their association with a putative coatomer complex I (Figure 6B, panel D); however, some distinct GFP-labeled vesicular structures, mostly but not exclusively in peripheral areas of the cell, were left intact and were apparently not affected by brefeldin A, indicating that they constitute a possible post-Golgi compartment.

Formation of Trafficking Compartments during Encystation of Giardia

In an attempt to visualize the developmental steps in CWP1 synthesis and transport during encystation of *Giardia*, we examined cells expressing the C4-GFP gene product at different time points after induction in vitro. A limiting factor in *Giardia* is the vigorous motility of live parasites, which severely restricts the time span during which cellular changes can be recorded. We therefore identified typical vesicular patterns for a given stage during differentiation in embedded cells. Twenty optical sections from cells representative of four stages of encystation were produced using a confocal laser scanning fluorescence microscope with appropriate filters and conditions for detection of DAPI, GFP, and DIC signals (Figure 7). Three-dimensional reconstruction of vesicular structures and nuclei in each cell was performed from the DAPI and GFP images (Figure 7, C, F, I, and L).

In parasites between 2 and 5 h after induction, we observed brightly fluorescent, tubular, or sheath-like structures in the vicinity of the nuclei (Figure 7, A–C). In some individual optical sections the nuclear circumference was completely outlined by GFP. Small vesicles, which were presumed to be early ESVs, in more peripheral areas had adopted a spherical shape. Approximately 5 h after induction, most cells showed larger spherical ESVs in addition to the perinuclear tubules, occupying a considerable volume of the cytoplasm (Figure 7, D–F). At 15 h an apparent condensation of GFP-labeled vesicular structures could be seen in the majority of the encysting parasites. A small number of large, closely grouped vesicles, in many cases two or three, but sometimes apparently only one major ESV, localized primarily to the anterior–dorsal part of the cells (Figure 7, G–I). Differential interference contrast images showed a clear outline of larger ESVs in optical sections that colocalized with the GFP signal (Figure 7, G and H). Vesicle condensation was accompanied by a marked reduction of the distinct perinuclear staining. Morphologically identifiable cyst walls were labeled by a strong GFP signal, and cells contained three to four identifiable nuclei (Figure 7J). We were unable to observe any intermediate stages representing encysting cells in the process of secreting the cyst wall material, suggesting that exocytosis, cyst wall formation, and the concomitant change to an ovoid shape of the nascent cysts are very rapid steps. Because of this, it remained unclear whether large, condensed ESVs in fact represent the ultimate step before exocytosis is initiated. Analysis of optical sections showed that no ESVs were present inside fully formed cysts, indicating that all the material had been secreted and presumably incorporated into the cyst wall (Figure 7, J and L). An alternative explanation for the lack of ESVs in cysts is that the contents of remaining vesicles that have failed to exocytose are subject to rapid degradation, possibly by fusion with the numerous lysosome-like peripheral vacuoles present near the dorsal surface. Interestingly, nuclear division was only observed after exocytosis of ESV contents, which is a further indication of a tight temporal regulation of the late stages of encystation, extending as far as the control of cell cycle progression.

DISCUSSION

In this study, a GFP-based assay system for the anaerobic parasite *Giardia duodenalis* was developed that allows stage-specific expression and tracking of newly synthesized GFP-tagged CWP1 as it progresses through the secretory pathway and is incorporated into the cyst wall. The results on expression kinetics of CWP1 indicate a tightly controlled synthesis of and accumulation of cyst wall proteins. Both positive regulation at the time of induction of encystation and negative regulation as CWP proteins accumulate appear to be involved, leading to the production of the appropriate amounts of CWP1.

Stage-specific regulation of gene expression in other medically important parasites accompanies crucial differentiation processes. These mark key points in the parasite life cycle (e.g., development of infectious stages) and as such offer attractive targets for intervention (Smith, 1995; McConville and Ralton, 1997; Barry *et al.*, 1998). The molecular basis of this regulation is still incompletely understood, however. In *Giardia* it was found that up-regulation of CWP1 mRNA expression during the formation of cysts occurs on the level of mRNA (Mowatt *et al.*, 1995; Lujan *et al.*, 1997), presumably via control of transcription initiation. Here we demonstrated that putative *cis*-DNA elements necessary and sufficient for control of CWP1 expression reside inside a small stretch of ~110 bp upstream of the CWP1 transcription initiation site, which is at position −11. The nucleotide sequence in this upstream flanking region is unremarkable, except for a short GC-rich sequence that is partially conserved in both CWP1 and CWP2. This sequence has been hypothesized to be a sterol regulatory element (Lujan *et al.*, 1997), involved in cholesterol-sensitive transcription regulation (Goldstein and Brown, 1990; Vallett *et al.*, 1996; Bist *et*

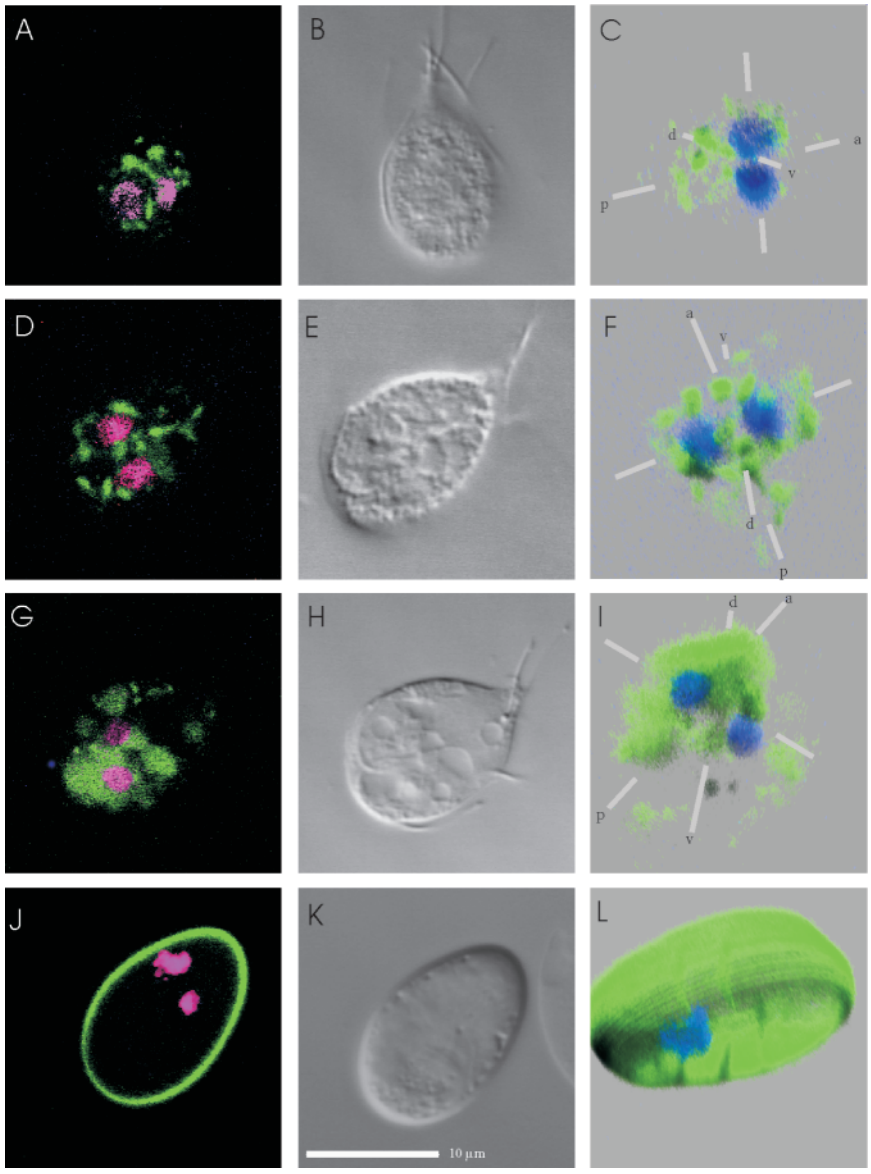

Figure 7. Intracellular localization of C4-GFP during four stages of encystation analyzed by confocal laser scanning microscopy: optical section 11 (A) (2.5 h after encystation), section 11 (D) (5 h), section 10 (G) (15 h), section 11 (J) (mature cyst), and corresponding DIC images (B, E, H, and K). Twenty optical sections were produced for each cell. Fluorescence images represent GFP signal (green) merged with DAPI signal (converted to red for better visibility) from a single centrally located optical section. All fluorescence images from each cell were used to calculate a three-dimensional representation (C, F, I, and L) showing encystation-specific vesicles and nuclei. The aspects of the three-dimensional images were chosen to provide an optimal view of GFP-labeled transport vesicles and nuclei and are indicated by white bars showing dorsal (d), ventral (v), anterior (a), and posterior (p) sides. Unlabeled lateral bars are also shown on each side.

al., 1997). Because CWP1 was not seen in the cytoplasm of mature cysts, negative regulation of CWP1 synthesis is required during the late stage of encystation. We found that in addition to the possible reduction of transcription initiation, regulation of mRNA stability may also be involved. Replacement of the CWP1 3′ flanking sequence with that of the constitutively expressed protein phosphatase 2C gene increased steady-state reporter mRNA levels ~40-fold during encystation. Our interpretation is that the 37 nt CWP1 3′UTR harbors a *cis*-acting element that targets the mRNA for degradation, either by reducing stability of the mature message directly or by altering the efficiency of posttranscriptional processing. This effect was independent of sequences in the coding region of CWP1. A possible contribution of the 11 nt 5′UTR, which was the only other CWP1-derived sequence in the mRNA tested, will have to be examined. Modulation of mRNA stability via *cis* motifs in the 3′UTR appears to be ubiquitous in cells that undergo differentiation and has been described in protozoa (Vanhamme and Pays, 1995), *Drosophila* (Surdej and Jacobs-Lorena, 1998), mammals (Mitchusson *et al.*, 1998), and other organisms. Particularly in protozoa, the sequence motifs responsible for interaction with putative *trans*-acting factors that influence mRNA instability have been difficult to pin down, because multiple and sometimes widely spaced regions are involved and consensus motifs are very degenerate (Furger *et al.*, 1997; Schurch *et al.*, 1997; Wilson *et al.*, 1999). Because untranslated flanking sequences are exceptionally short in *Giardia*, this organism could therefore serve as a valuable model for the elucidation of the molecular basis for this type of regulation.

The *Giardia* cyst wall is composed of protein and a large proportion of carbohydrate (~40%), mainly in the form of *N*-acetylgalactosamine and a small number of other sugars. How these components are complexed has not been deter-

mined, but the final fibrillar extracellular matrix observed in electron microscopy points to a highly organized structure involving extensive protein–protein interactions (Erlandsen *et al.*, 1989). CWP1 and CWP2 have been shown to associate covalently within 5 min of their synthesis via disulfide bridges (Lujan *et al.*, 1995b). It was speculated that the C-terminal domain of CWP1 and the homologous region in CWP2 containing seven cysteines each are likely to be involved in the formation of heterodimers. In Western blot experiments, we found evidence for the involvement of cysteines in at least two domains of CWP1 promoting covalent interaction with other proteins, presumably with CWP2. The increased stability with progressive addition of CWP1 sequences, together with the faithful incorporation of the C3-GFP protein into the cyst wall, makes it likely that the recombinant CWP1–GFP chimeras indeed form specific heterodimers with endogenous proteins. Results with the C2-GFP reporter show that the presence of domain II containing three cysteines is not sufficient to create a stable link to other cyst wall components that will persist on the extracellular side of the plasma membrane. Inclusion of CWP1 domain IV in the chimera, however, resulted in a marked stabilization of covalent intermolecular association, confirming its role in the formation of heterodimeric structures. Stable association and incorporation of C3-GFP into the cyst wall occurred in the absence of domain IV and may be mediated by a direct interaction with other as yet unidentified cyst wall components via LRRs. LRR containing proteins are found across the prokaryotic–eukaryotic border (Kobe and Deisenhofer, 1995a), fulfilling a vast range of functions involving protein–protein interactions (Kobe and Deisenhofer, 1995b). Among these, proteins with adhesive properties, e.g., decorin and fibromodulin, which regulate collagen fibril formation (Kresse *et al.*, 1993), constitute a large subfamily with binding sites in the extracellular matrix. The versatile and flexible LRR modules are thought to play a structural role in assisting the formation of multimers. Our data indicate that in *Giardia* the CWP LRRs may play a similar role in forming the final fibrillar extracellular matrix during maturation of the secreted cyst wall material, and as such constitute critical structural components of these proteins.

The use of GFP as a reporter to explore secretory transport in anaerobic organisms is inherently difficult and has not been documented previously. Molecular oxygen is required during posttranslational maturation of GFP to dehydrogenate the α, β-bond of residue 66 (Heim *et al.*, 1994; Reid and Flynn, 1997). In *Giardia* expressing GFP, fluorescence was virtually absent upon harvesting but was vastly improved after exposing the cells to oxygen at temperatures around 2°C. This demonstrated that GFP inside vesicles of the secretory pathway as well as on the cell surface can unfold sufficiently at these lower temperatures to allow oxygenation with limited damage to the cells. Cooling of *Giardia* trophozoites from 37°C to temperatures below 4°C blocks action of the sucking disk and is standard procedure for harvesting adherent parasites for passage. Oxygenation at room temperature and 37°C, on the other hand, was detrimental to the parasites. As an added benefit, exposure to atmospheric oxygen in the cold allows observation of fluorescently labeled, live parasites after the temperature is raised to 37°C again in anaerobic conditions. We have used a GFP variant (m-GFP-5) (Siemering *et al.*, 1996) that had been mutated to improve protein folding at 37°C. This apparently did not impair the ability of the "thermoresistant" form of GFP to complete maturation also at lower temperatures.

Our microscopy data show that late ESVs are condensed into very few or even a single membrane-bound compartment of irregular shape, representing most likely large storage vesicles for cyst wall material. This result raises several questions regarding the mechanism of deposition of the cell wall components. Previous work has shown that ESV membranes can become continuous with the plasma membrane, suggesting that ESV contents are secreted by exocytosis (Reiner *et al.*, 1990). On the other hand, scanning electron microscopy has shown the presence of numerous knob-like structures on the plasma membrane and even on flagella of encysting cells that react with an antibody specific for cyst wall components and were postulated to be the attachment points for the fibrils observed on mature cyst walls (Erlandsen *et al.*, 1996). Outgrowth of fibrils from many different locations on the plasma membrane, however, has not been demonstrated and would be difficult to reconcile with the localization of the membrane-bound ESVs that we see before deposition of the cyst wall. Because exocytosis appears to be a very rapid step, as intermediates in the process of cyst wall deposition could not be identified, determination of the exact shape and localization of the ESVs immediately before secretion will require further study. On the basis of our data, we favor the hypothesis that the ESV contents are secreted at one or several points by exocytosis and disperse laterally until the entire cell is engulfed. To access and fuse with the surface membrane, the large ESVs may possibly fragment again into smaller vesicles that are actively transported to different locations beneath the plasma membrane before exocytosis.

The properties of regulated transport during *Giardia* encystation, other than its vesicular nature, are poorly understood. Recent work indicates that bona fide Golgi function (Lujan *et al.*, 1995a; Das and Gillin, 1996), and to some extent also morphology (McCaffery and Gillin, 1994), is present only in encysting *Giardia* parasites. Because such stage-specificity of the protein transport machinery is not known in any other organism, this would make encysting *Giardia* a unique model for studying neogenesis of certain Golgi structures. By labeling Golgi membranes with BODIPY-TR–ceramide, we showed that GFP-tagged CWP1 colocalized with a previously observed perinuclear structure (Lujan *et al.*, 1997), which is intensely labeled by the marker lipid. Although endomembranes were also seen in trophozoites, perinuclear accumulation of Golgi membranes was not observed. It remains to be determined whether increase of membrane compartments during *Giardia* encystation is due to de novo synthesis of an "encystation-specific Golgi" or, alternatively, an amplification of compartments already present in trophozoites, as has been observed in transgenic Madin–Darby canine kidney cells that overexpress human growth hormone (Rudick *et al.*, 1993). Considering the large amounts of newly produced cyst wall material that have to be accommodated, the latter explanation is certainly the simpler one. More significantly, the membranes of some peripheral vesicles containing GFP–CWP1 were not stained, or were only partially stained, with BODIPY-TR–ceramide. We take this as an indication that these ESVs belong to a

putative *trans*-Golgi network or constitute specialized secretory and/or storage compartments for cyst wall material. In support of this notion, we also observed labeled vesicles that were resistant to treatment with brefeldin A in transgenic encysting cells, indicating that they were not associated with coatomer complex I and thus not part of a Golgi compartment. Although these experiments provide no rigorous proof that CWPs pass through the *Giardia* Golgi, they are suggestive of a protein transport machinery with characteristics similar to those of more highly developed eukaryotes; however, clarification of the exact nature of ESVs and detailed investigation of the complex processes involved in the establishment of the *Giardia* cyst wall will require further development of the molecular tools presented herein, as well as identification and localization of *Giardia*-specific markers for secretory compartments.

ACKNOWLEDGMENTS

Our thanks go to Drs. M. Höchli and T. Bächi (Elektronenmikroskopisches Zentrallaboratorium, Universität Zürich) for excellent technical assistance with confocal microscopy. We are also indebted to Drs. J.-H. Tai and K. Kim for help with establishing *Giardia* transfection and GFP expression, and to Dr. A. Schneider for critical reading of the manuscript. This work was supported by the Swiss National Science Foundation (grants 31-45841.95 and 31-58912.99).

REFERENCES

Adam, R.D. (1991). The biology of Giardia spp. Microbiol. Rev. *55,* 706–732.

Ausubel, F.M., Brent, R., Kingston, R.E., Moore, D.D., Seidman, J.G., Smith, J.A., and Struhl, K. (1994). Current Protocols in Molecular Biology, vol. 2, New York: John Wiley & Sons.

Barry, J.D., Graham, S.V., Fotheringham, M., Graham, V.S., Kobryn, K., and Wymer, B. (1998). VSG gene control and infectivity strategy of metacyclic stage Trypanosoma brucei. Mol. Biochem. Parasitol. *91,* 93–105.

Bist, A., Fielding, P.E., and Fielding, C.J. (1997). Two sterol regulatory element-like sequences mediate up-regulation of caveolin gene transcription in response to low density lipoprotein free cholesterol. Proc. Natl. Acad. Sci. USA *94,* 10693–10698.

Boucher, S.E., and Gillin, F.D. (1990). Excystation of in vitro-derived Giardia lamblia cysts. Infect. Immun. *58,* 3516–3522.

Bruderer, T., Papanastasiou, P., Castro, R., and Köhler, P. (1993). Variant cysteine-rich surface proteins of Giardia isolates from human and animal sources. Infect. Immun. *61,* 2937–2944.

Bulik, D.A., Lindmark, D.G., and Jarroll, E.L. (1998). Purification and characterization of UDP-*N*-acetylglucosamine pyrophosphorylase from encysting Giardia. Mol. Biochem. Parasitol. *95,* 135–139.

Chen, L.M., Chern, Y., Ong, S.J., and Tai, J.H. (1994). Molecular cloning and characterization of a ras-related gene of ran/tc4/spi1 subfamily in Giardia lamblia. J. Biol. Chem. *269,* 17297–17304.

Das, S., and Gillin, F.D. (1996). Giardia lamblia: increased UDP-*N*-acetyl-D-glucosamine and *N*-acetyl-D-galactosamine transferase activities during encystation. Exp. Parasitol. *83,* 19–29.

Drouin, G., Moniz de Sa, M., and Zuker, M. (1995). The Giardia lamblia actin gene and the phylogeny of eukaryotes. J. Mol. Evol. *41,* 841–849.

Dubey, J.P., Lindsay, D.S., and Speer, C.A. (1998). Structures of Toxoplasma gondii tachyzoites, bradyzoites, and sporozoites and biology and development of tissue cysts. Clin. Microbiol. Rev. *11,* 267–299.

Eichinger, D. (1997). Encystation of Entamoeba parasites. BioEssays *19,* 633–639.

Ellis, J.E., Wyder, M.A., Jarroll, E.L., and Kaneshiro, E.S. (1996). Changes in lipid composition during in vitro encystation and fatty acid desaturase activity of Giardia lamblia. Mol. Biochem. Parasitol. *81,* 13–25.

Erlandsen, S.L., Bemrick, W.J., and Pawley, J. (1989). High-resolution electron microscopic evidence for the filamentous structure of the cyst wall in Giardia muris and Giardia duodenalis. J. Parasitol. *75,* 787–797.

Erlandsen, S.L., Macechko, P.T., van Keulen, H., and Jarroll, E.L. (1996). Formation of the Giardia cyst wall: studies on extracellular assembly using immunogold labeling and high resolution field emission SEM. J. Eukaryot. Microbiol. *43,* 416–429.

Furger, A., Schürch, N., Kurath, U., and Roditi, I. (1997). Elements in the 3′ untranslated region of procyclin mRNA regulate expression in insect forms of Trypanosoma brucei by modulating RNA stability and translation. Mol. Cell. Biol. *17,* 4372–4380.

Goldstein, J.L., and Brown, M.S. (1990). Regulation of the mevalonate pathway. Nature *343,* 425–430.

Gupta, R.S., Aitken, K., Falah, M., and Singh, B. (1994). Cloning of Giardia lamblia heat shock protein HSP70 homologs: implications regarding origin of eukaryotic cells and of endoplasmic reticulum. Proc. Natl. Acad. Sci. USA *91* 2895–2899.

Heim, R., Prasher, D.C., and Tsien, R.Y. (1994). Wavelength mutations and posttranslational auto-oxidation of green fluorescent protein. Proc. Natl. Acad. Sci. USA *91,* 12501–12504.

Knodler, L.A., Svard, S.G., Silberman, J.D., Davids, B.J., and Gillin, F.D. (1999). Developmental gene regulation in Giardia lamblia: first evidence for an encystation-specific promoter and differential 5′ mRNA processing. Mol. Microbiol. *34,* 327–340.

Kobe, B., and Deisenhofer, J. (1995a). Proteins with leucine-rich repeats. Curr. Opin. Struct. Biol. *5,* 409–416.

Kobe, B., and Deisenhofer, J. (1995b). A structural basis of the interactions between leucine-rich repeats and protein ligands. Nature *374,* 183–186.

Kresse, H., Hausser, H., and Schonherr, E. (1993). Small proteoglycans. Experientia *49,* 403–416.

Leipe, D.D., Gunderson, J.H., Nerad, T.A., and Sogin, M.L. (1993). Small subunit ribosomal RNA+ of Hexamita inflata and the quest for the first branch in the eukaryotic tree. Mol. Biochem. Parasitol. *59,* 41–48.

Lujan, H.D., Marotta, A., Mowatt, M.R., Sciaky, N., Lippincott-Schwartz, J., and Nash, T.E. (1995a). Developmental induction of Golgi structure and function in the primitive eukaryote Giardia lamblia. J. Biol. Chem. *270,* 4612–4618.

Lujan, H.D., Mowatt, M.R., Conrad, J.T., Bowers, B., and Nash, T.E. (1995b). Identification of a novel Giardia lamblia cyst wall protein with leucine-rich repeats. Implications for secretory granule formation and protein assembly into the cyst wall. J. Biol. Chem. *270,* 29307–29313.

Lujan, H.D., Mowatt, M.R., and Nash, T.E. (1997). Mechanisms of Giardia lamblia differentiation into cysts. Microbiology *61,* 294–304.

Manning, P., Erlandsen, S.L., and Jarroll, E.L. (1992). Carbohydrate and amino acid analyses of Giardia muris cysts. J. Protozool. *39,* 290–296.

McCaffery, J.M., and Gillin, F.D. (1994). Giardia lamblia: ultrastructural basis of protein transport during growth and encystation. Exp. Parasitol. *79,* 220–235.

McConville, M.J., and Ralton, J.E. (1997). Developmentally regulated changes in the cell surface architecture of Leishmania parasites. Behring Inst. Mitt. 34–43.

Mitchusson, K.D., Blaxall, B.C., Pende, A., and Port, J.D. (1998). Agonist-mediated destabilization of human beta1-adrenergic receptor mRNA: role of the 3′ untranslated translated region. Biochem. Biophys. Res. Commun. *252,* 357–362.

Mowatt, M.R., Lujan, H.D., Cotten, D.B., Bowers, B., Yee, J., Nash, T.E., and Stibbs, H.H. (1995). Developmentally regulated expression of a Giardia lamblia cyst wall protein gene. Mol. Microbiol. *15,* 955–963.

Pagano, R.E. (1989). A fluorescent derivative of ceramide: physical properties and use in studying the Golgi apparatus of animal cells. Methods Cell Biol. *29,* 75–85.

Pagano, R.E., and Martin, O.C. (1988). A series of fluorescent *N*-acylsphingosines: synthesis, physical properties, and studies in cultured cells. Biochemistry *27,* 4439–4445.

Paget, T.A., Macechko, P.T., and Jarroll, E.L. (1998). Metabolic changes in Giardia intestinalis during differentiation. J. Parasitol. *84,* 222–226.

Que, X., Svard, S.G., Meng, T.C., Hetsko, M.L., Aley, S.B., and Gillin, F.D. (1996). Developmentally regulated transcripts and evidence of differential mRNA processing in Giardia lamblia. Mol. Biochem. Parasitol. *81,* 101–110.

Reid, B.G., and Flynn, G.C. (1997). Chromophore formation in green fluorescent protein. Biochemistry *36,* 6786–6791.

Reiner, D.S., Douglas, H., and Gillin, F.D. (1989). Identification and localization of cyst-specific antigens of Giardia lamblia. Infect. Immun. *57,* 963–968.

Reiner, D.S., Hetsko, M.L., Das, S., Ward, H.D., McCaffery, M., and Gillin, F.D. (1993). Giardia lamblia: absence of cyst antigens and reduced secretory vesicle formation and bile salt uptake in an encystation-deficient subline. Exp. Parasitol. *77,* 461–472.

Reiner, D.S., McCaffery, M., and Gillin, F.D. (1990). Sorting of cyst wall proteins to a regulated secretory pathway during differentiation of the primitive eukaryote, Giardia lamblia. Eur. J. Cell Biol. *53,* 142–153.

Roger, A.J., Morrison, H.G., and Sogin, M.L. (1999). Primary structure and phylogenetic relationships of a malate dehydrogenase gene from Giardia lamblia. J. Mol. Evol. *48,* 750–755.

Rudick, V.L., Rudick, M.J., and Brun-Zinkernagel, A.M. (1993). Amplification of the Golgi complex in MDCK cells secreting human growth hormone. J. Cell Sci. *104,* 509–520.

Schürch, N., Furger, A., Kurath, U., and Roditi, I. (1997). Contributions of the procyclin 3′ untranslated region and coding region to the regulation of expression in bloodstream forms of Trypanosoma brucei. Mol. Biochem. Parasitol. *89,* 109–121.

Siemering, K.R., Golbik, R., Sever, R., and Haseloff, J. (1996). Mutations that suppress the thermosensitivity of green fluorescent protein. Curr. Biol. *6,* 1653–1663.

Singer, S.M., Yee, J., and Nash, T.E. (1998). Episomal and integrated maintenance of foreign DNA in Giardia lamblia. Mol. Biochem. Parasitol. *92,* 59–69.

Smith, J.E. (1995). A ubiquitous intracellular parasite: the cellular biology of Toxoplasma gondii. Int. J. Parasitol. *25,* 1301–1309.

Smith, P.D., Gillin, F.D., Spira, W.M., and Nash, T.E. (1982). Chronic giardiasis: studies on drug sensitivity, toxin production, and host immune response. Gastroenterology *83,* 797–803.

Sogin, M.L., Gunderson, J.H., Elwood, H.J., Alonso, R.A., and Peattie, D.A. (1989). Phylogenetic meaning of the kingdom concept: an unusual ribosomal RNA from Giardia lamblia. Science *243,* 75–77.

Steimle, P.A., Lindmark, D.G., and Jarroll, E.L. (1997). Purification and characterization of encystment-induced glucosamine 6-phosphate isomerase in Giardia. Mol. Biochem. Parasitol. *84,* 149–153.

Sun, C.H., Chou, C.F., and Tai, J.H. (1998). Stable DNA transfection of the primitive protozoan pathogen Giardia lamblia. Mol. Biochem. Parasitol. *92,* 123–132.

Surdej, P., and Jacobs-Lorena, M. (1998). Developmental regulation of bicoid mRNA stability is mediated by the first 43 nucleotides of the 3′ untranslated region. Mol. Cell. Biol. *18,* 2892–2900.

Taratuto, A.L., and Venturiello, S.M. (1997). Echinococcosis. Brain Pathol. *7,* 673–679.

Vallett, S.M., Sanchez, H.B., Rosenfeld, J.M., and Osborne, T.F. (1996). A direct role for sterol regulatory element binding protein in activation of 3-hydroxy-3-methylglutaryl coenzyme A reductase gene. J. Biol. Chem. *271,* 12247–12253.

Vanhamme, L., and Pays, E. (1995). Control of gene expression in trypanosomes. Microbiol. Rev. *59,* 223–240.

Van Keulen, H., Steimle, P.A., Bulik, D.A., Borowiak, R.K., and Jarroll, E.L. (1998). Cloning of two putative Giardia lamblia glucosamine 6-phosphate isomerase genes only one of which is transcriptionally activated during encystment. J. Eukaryot. Microbiol. *45,* 637–642.

Wang, A.L., Sepp, T., and Wang, C.C. (1995). Electroporation in Giardia lamblia. Methods Mol. Biol. *47,* 361–367.

Wilson, K., Uyetake, L., and Boothroyd, J. (1999). Trypanosoma brucei: cis-acting sequences involved in the developmental regulation of PARP expression. Exp. Parasitol. *91,* 222–230.

Yee, J., and Nash, T.E. (1995). Transient transfection and expression of firefly luciferase in Giardia lamblia. Proc. Natl. Acad. Sci. USA *92,* 5615–5619.

Yu, D.C., Wang, A.L., and Wang, C.C. (1996a). Amplification, expression, and packaging of a foreign gene by giardiavirus in Giardia lamblia. J. Virol. *70,* 8752–8757.

Yu, D.C., Wang, A.L., and Wang, C.C. (1996b). Stable coexpression of a drug-resistance gene and a heterologous gene in an ancient parasitic protozoan Giardia lamblia. Mol. Biochem. Parasitol. *83,* 81–91.

Yu, D.C., Wang, A.L., Wu, C.H., and Wang, C.C. (1995). Virus-mediated expression of firefly luciferase in the parasitic protozoan Giardia lamblia. Mol. Cell. Biol. *15,* 4867–4872.